

Paper:

# Structure Deformation Measurement with Terrestrial Laser Scanner at Pathein Bridge in Myanmar

Nuntikorn Kitratporn<sup>†</sup>, Wataru Takeuchi, Koji Matsumoto, and Kohei Nagai

Institute of Industrial Science, The University of Tokyo  
Komaba, Meguro-ku, Tokyo, Japan

<sup>†</sup>Corresponding author, E-mail: tita@iis.u-tokyo.ac.jp

[Received September 1, 2017; accepted January 16, 2018]

In Myanmar, defects and possible deformation were reported in many long-span suspension bridges. The current state of bridge infrastructure must be inspected, so that deterioration can be stalled and failure can be prevented. A 3D laser scanner, specifically the terrestrial laser scanner (TLS), has demonstrated the ability to capture surface geometry with millimeter accuracy. Consequently, TLS technology has received significant interest in various applications including in the field of structural survey. However, research on its application in large bridge structure remains limited. This study examines the use of TLS point cloud for the measurement of three deformation behaviors at the Pathein Suspension Bridge in Myanmar. These behaviors include tower inclination, hanger inclination, and deflection of bridge truss. The measurement results clearly captured the deformation state of the bridge. A comparison of the measurement results with available conventional measurements yielded overall agreement. However, errors were observed in some areas, which could be due to noise and occlusion in the point cloud model. In this study, the advantages of TLS in providing non-discrete data, direct measurement in meaningful unit, and access to difficult-to-access sections, such as top of towers or main cables, were demonstrated. The limitations of TLS as observed in this study were mainly influenced by external factors during field survey. Hence, it was suggested that further study on appropriate TLS surveying practice for large bridge structure should be conducted.

**Keywords:** bridge inspection, geometric measurement, terrestrial laser scanner, point cloud, 3D model

## 1. Study Site and Methodology

## 2. Introduction

Being a modern lifeline structure, the collapse of major bridges can lead to local-scale disaster resulting in casualties and substantial economic loss. Bridge inspection is perceived as a crucial step for further maintenance decision, which can prevent bridge failure. Myanmar has the

second largest geographical area in Southeast Asia and in recent years, the fastest growing economy in the region. Rapid urban expansion and economic development brings about a push for improvement in transport infrastructure. The construction of new roads and bridges have been carried out and this trend is expected to continue. As of 2012, Myanmar has a total of 4,728 bridges of which 741 bridges were considered major bridges spanning 54 m or longer [1]. However, existing bridges have been reported with signs of deformation and deterioration requiring proper reinforcement and maintenance [2]. Therefore, inspection of these bridge is necessary.

Recent interest in structural survey focuses on terrestrial laser scanner (TLS), a mid-range ground-based 3D laser scanning system. TLS technology can record surface geometry of object of interest without direct contact and generate a high-precision model in millimeter accuracy. The basic output of TLS survey is a set of points with each point containing coordinates of its location in space. This output is called point cloud. The advantages and need for 3D structural information was emphasized by Park et al. [3]. The potential applications of TLS are in fields such as engineering [4, 5], architecture [6], forestry [7, 8], and heritage [9]. Various structural related studies have attempted to utilize TLS technology, such as structural deformation assessment [10, 11], and bridge surface damage detection [12]. However, these studies were either conducted within laboratory settings or on a small-scale structure. Few studies have applied TLS for the survey of large structures. Pesci et al. [13] proposed a method to measure 35-100 m height masonry structure deformation by computing the differences between TLS data and a numerically constructed plane. Oskouie et al. [14] analyzed the displacement of a highway retaining wall using TLS point cloud. Still, the application of TLS for long span bridges remains unexplored.

The objective of this study is to measure deformation of a bridge structure using TLS point cloud. The Pathein Bridge, a single span suspension bridge, was selected as a study site. Data was collected at the site using TLS station from FARO and three deformation behaviors were of interest for measurement. These behaviors include 1) tower inclination, 2) hanger inclination, and 3) truss or deck deflection. The results were compared to available conventional measuring methods. The advantages and limi-

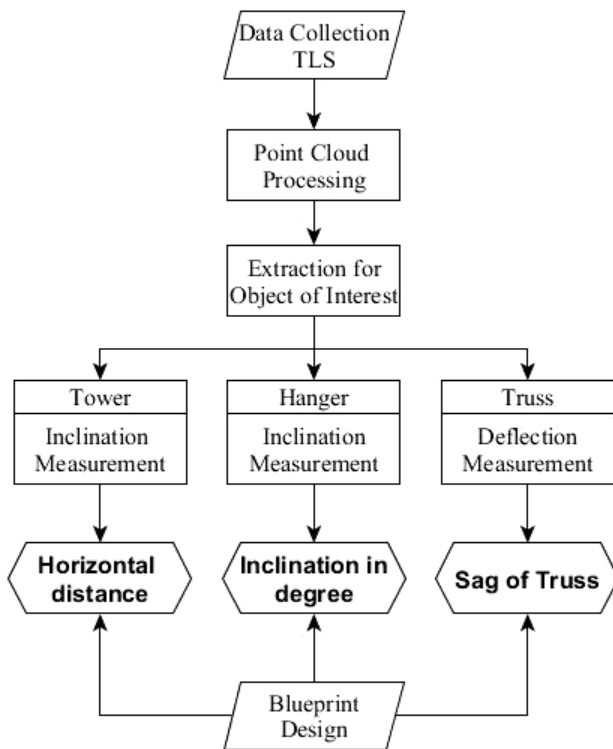


Fig. 3. Workflow to measure deformation from TLS point cloud.

tations of TLS point cloud to measure the current state of bridge structure were also identified.

### 2.1. Pathein Bridge Conditions

The Pathein Bridge was constructed in 2004 across the Pathein river between Pathein township and Ngwesaung township. Its location and design blueprint are shown in Fig. 1. The bridge is located approximately 200 km from Yangon, the largest city in Myanmar. It is the nearest bridge connecting Yangon to the coastal towns on the west side of the country. The bridge's total span is 458.22 m, comprising 268.22 m main span and 86 m approaching span measured from the anchorage on each side. Its towers were constructed with a steel segment erected 30.54 m on top of reinforced concrete piers. The main deck is supported by 104 hangers, 52 on each side.

Visual inspection was performed and various defects of the bridge were reported [1]. The road surface is situated in an abnormal shape (Fig. 2a). Concrete cracks along the cross beam of approaching pillars were also present (Fig. 2b). Investigations by the Ministry of Construction (MOC) did not indicate when these symptoms occurred or reasons behind them. However, it was suggested that the observed defects indicate possible deformation of the bridge.

### 2.2. Data Collection and Point Cloud Processing

The overall methodology is shown in Fig. 3. This section provides information on the field survey and preparation of the point cloud from surveyed data. The finished

point cloud was then extracted for measurement, as presented in Sections 2.3 and 2.4.

On-site measurement at the Pathein Bridge was carried out on the 7<sup>th</sup> and 8<sup>th</sup> of February, 2017. February, a dry season, was selected owing to low occlusion from vegetation and accessibility to the base of the bridge tower, which may otherwise be muddy. In this study, a medium-range, phase-shift laser scanner, Faro Focus3D X330, was used. The device can measure up to 330 m with 360° horizontal and 330° vertical field of view. The range error of the laser measurement is 2 mm at 25 m from the scanner. Parameters on the device that affect details of the scan results and scanning duration include scan resolution, scan quality, and scan field of view. The field of view was not adjusted and the default 360° horizontal and 330° vertical field of view was used for ease of setup during the field survey. The resolution determines the density and distance of points, while the quality determines the time used for point sampling. High resolution provides sharper details, while higher quality provides less noise. In this survey, 1/2 resolution with 2x quality were used. These settings approximately yield a point distance of 3 mm at 10 m from the scanner. Furthermore, a scan speed of 488,000 points per second was achieved in approximately 15 minutes per scan. High resolution was selected to ensure adequate number of points for the objects of interest, in this case the hanger, which are considerably small and located far from the scanner. This is useful to compensate the reduction of point density representing distant objects as laser beams travel further from the scanner.

TLS is a line-of-sight equipment, which means that such device cannot collect data behind obstruction. Hence, multiple scans from different angles are usually required to capture the entire structure. Survey targets were not distributed because traffic cannot be halted and high-reach devices were not available. For this survey, a total of 20 scans were carried out. Seven scan locations were completed around the main tower on each side and 6 scan locations were completed on the deck section. One scan was removed due to occlusion from large tree located next to T2 tower. The scanning locations are shown in Fig. 4a. An example of a single scanned point cloud from a scanner view point is shown in Fig. 4b.

Collected data was processed using Faro SCENE software. The specified device error from manufacturer is 2 mm. However, additional errors can occur during field survey. Dark scan and edge artifact are commonly known errors. Dark scan occurs when laser beams hit a highly reflective object, while edge artifact can result from multiple factors, such as multiple returns of different range objects along a single laser beam. Details of these errors were discussed by Sotoodeh [15]. To reduce uncertainty due to the aforementioned errors, filtering functions on SCENE was applied on each raw scan. Dark scan point filtering removes all points under a certain reflectance value. Stray point filtering and edge artifact filtering remove outliers resulting from edge effects. Applying filtering can decrease noise and improve quality, such that higher accuracy can be obtained in later processing.

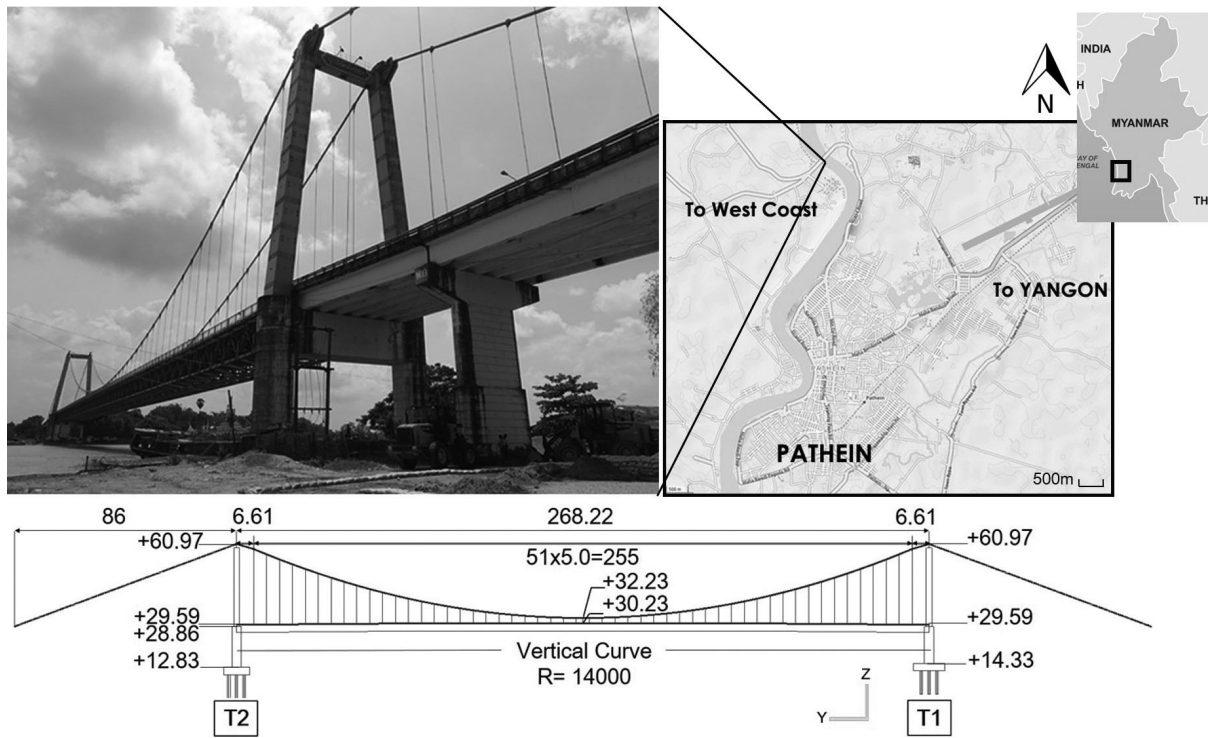


**Fig. 1.** Pathein bridge location ( $16^{\circ}49'27.3''$  N  $94^{\circ}43'55.9''$  E) and design drawing (elevations and dimensions are given in meter).



**Fig. 2.** Defects identified from previous visual inspection: (a) Road surface with abnormal shape where the middle deck is situated lower than the design. (b) Concrete crack at the cross beam imply possible movement of the main deck section

After removing outliers, each raw scan is required to be co-registered to create a single combined model. Each raw scan is referenced to the location of the scanner at the time the scan was done. TLS is equipped with GPS, which assists in identifying scan locations. Nevertheless, it only provides a rough guideline. In this study, co-registration was completed by target-less registration using unique structural features with no or minimal positional change; then, cloud-to-cloud optimization method was applied. This cloud-based optimization is based on an algorithm in which one scan is fixed while the other scan is shifted and rotated to minimize the distance between the closest point in each scan. Finally, duplicate point removal and homogenize point density were set to minimize

the size of the finished model and memory requirement during visualize. A spacing of 5 mm between points was selected. A local coordinate was also created by applying planner alignment using the planer surface of the cross-beam at T1 tower. The local coordinate was setup so that  $x$ -axis represents the lateral bridge direction,  $y$ -axis represents the longitudinal bridge direction, and  $z$ -axis represents the elevation. To reduce additional time required for applying the RBG image, the final point cloud did not contain color as shown in **Fig. 4c**.

### 2.3. Object of Interest Extraction

The final point cloud model includes surrounding objects that are not relevant to our measurement, such as

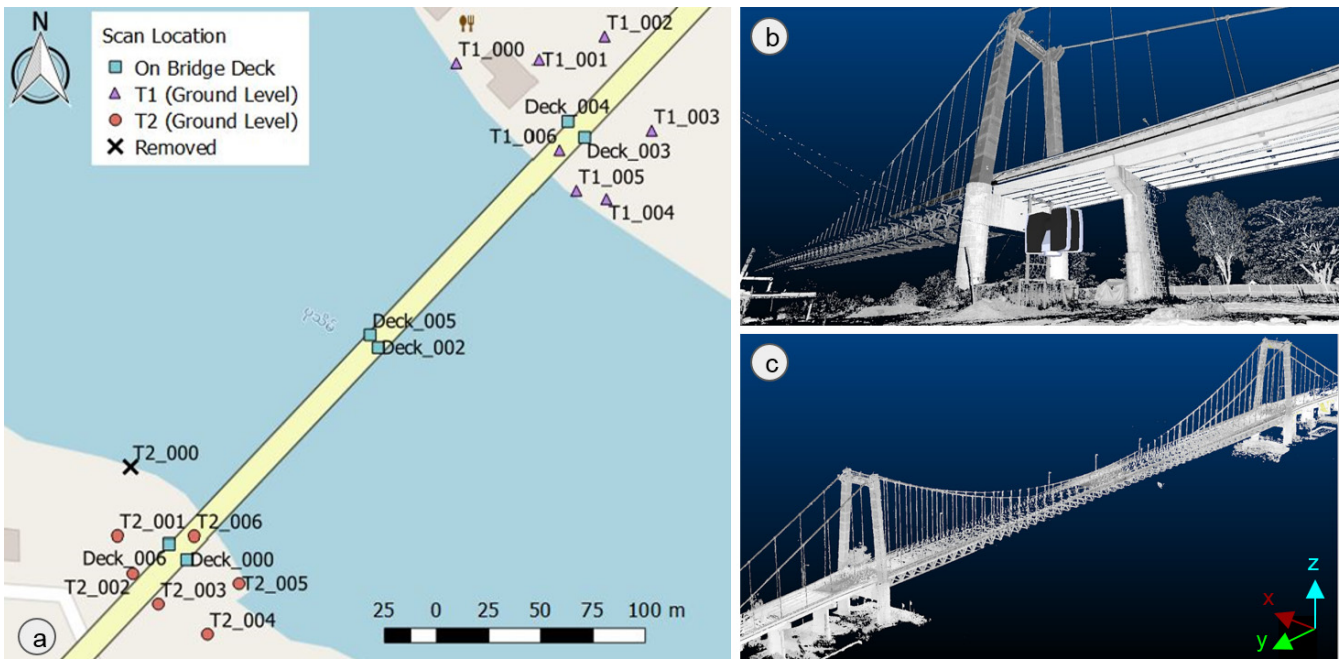


Fig. 4. (a) Overview of the scan location. (b) Example of a single scan from a view point of T1\_003 scan location. (c) Combined point cloud after co-registration.

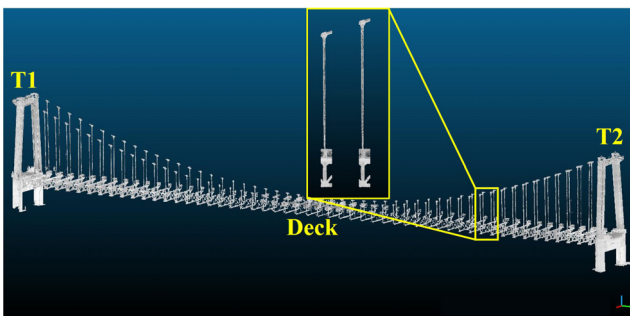


Fig. 5. Extracted point cloud of T1, T2, and deck sections.

trees and buildings. The objects of interest can be extracted using clipping box based on visual interpretation or prior knowledge on structure dimension. Tower T1 and T2 were extracted by visual evaluation into 2 separate models. The extraction of bridge deck portion was performed based on consistent distance between each hanger located along the longitudinal direction of the bridge. Clipping boxes with  $20.25 \times 1.4 \times 36.0$  m in  $x$ ,  $y$ , and  $z$  were created at every 5.5 m interval along the longitudinal direction of the bridge. Each clipping box contains a pair of upstream and downstream hangers. The extracted point cloud for T1, T2, and deck are shown in Fig. 5.

## 2.4. Measurement

### 2.4.1. Tower Inclination

Each measurement step for tower inclination is shown in Fig. 6.

*Step1* is to extract the planer surface that represents the steel tower. The pier section does not exhibit deformation. Hence, our measurement focused on the steel tower section. Since the steel tower is a rigid object,

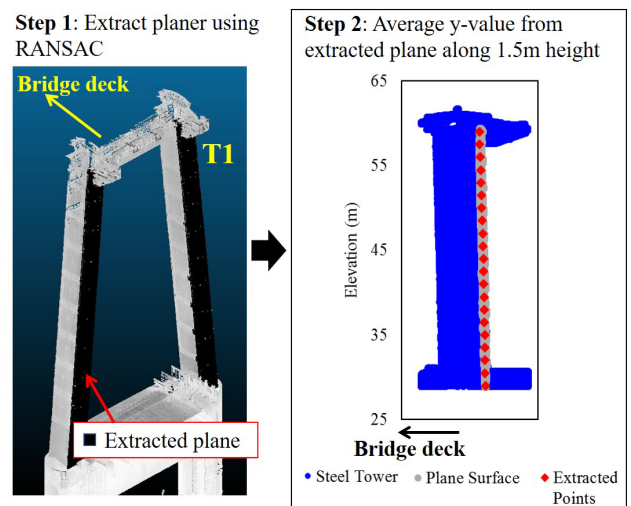


Fig. 6. Inclination measurement of main towers.

instead of using all 4 facets, a single surface can represent the characteristic of the tower. The facet located toward approaching span was selected because it gives the highest point density with minimal occlusion or missing points. Planers were extracted based on the RANSAC (RANdom Sample Consensus) algorithm developed by Wahl and Klein [16] because of its high tolerance against noise [17]. The RANSAC algorithm was set with a minimum of 200,000 points per each planer and 0.25 cm maximum distance to the best-fitting plane.

*Step2* averages the  $y$ -value of each point on the extracted planer within 1.5 m increment from 29 m elevation up to 59 m elevation.

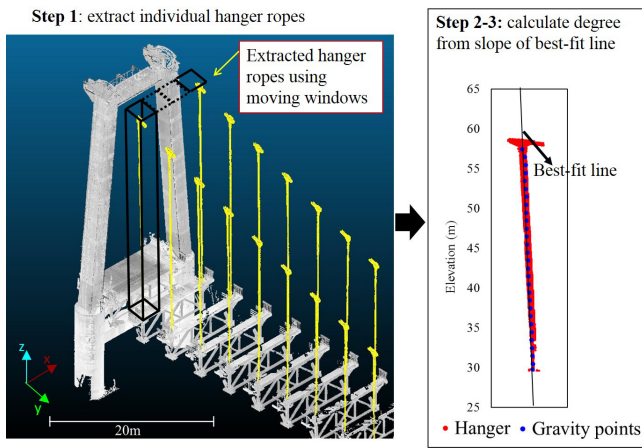


Fig. 7. Inclusion measurement of hangers.

### 2.4.2. Hanger Inclination

Each measurement step for hanger rope inclination is shown in Fig. 7.

Step1 is to retrieve the individual hanger rope. Point distribution in  $z$  and  $x$  axes was applied. The road surface is expected to contain a high number of points due to its close distance to the scanner. Hence, high number of points from the distribution curve plotted along  $z$ -axis can be used as a tool to extract points for hangers located above the road surface. Similarly, when plotted along the  $x$ -axis, the number of points representing a hanger is expected to be higher than the rest and kept. On extracted points, moving windows with  $2.5 \times 2.5$  m in  $x$  and  $y$  direction searched from minimum  $x$  and  $y$  points. If points exist inside a moving window, the  $z$  column is extracted.

Step2 is to calculate gravity points by averaging  $x$  and  $y$  values every 10cm increment along the  $z$ -axis. Based on the design of the bridge, the connection between the hanger rope and the road surface is fixed. Hence, the  $x$ -value and  $y$ -value from the lowest point were used as reference.

In Step3, the best-fit linear line was computed for displacement in the  $y$ -axis and height. The slope ( $l$ ) from the fitted line was then converted into degree using  $\theta = \tan^{-1}(l)$ .

Conventional measurement for hanger inclination was carried out using hand-held digital spirit level device on the same day as the TLS survey (Fig. 8). The digital spirit level used was a 9-inch terpedo level, and it provides accuracy of up to  $\pm 0.05^\circ$ .

### 2.4.3. Truss Deflection

Figure 9 illustrates each measurement step for truss deflection.

The inclination of each hanger rope along the bridge's longitudinal direction presented in degrees is plotted in Fig. 10. The hangers exhibited clear inclination only along the bridge's axis direction. At each end close to the main towers, the first three to four hangers were inclined toward the direction of their closest tower. The four hangers closest to T1 were inclined toward T1 direction, while



Fig. 8. Conventional measurement using digital spirit level for comparison with TLS results.

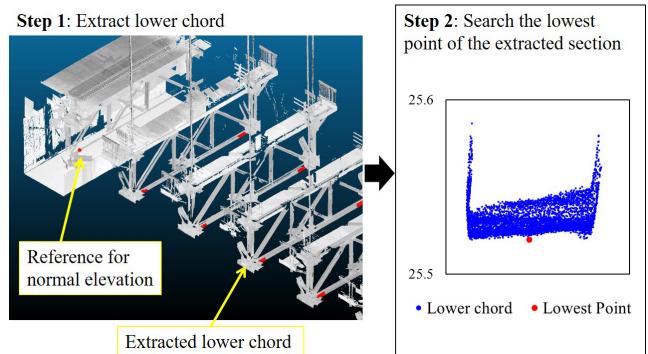


Fig. 9. Steps for deflection measurement of bridge truss.

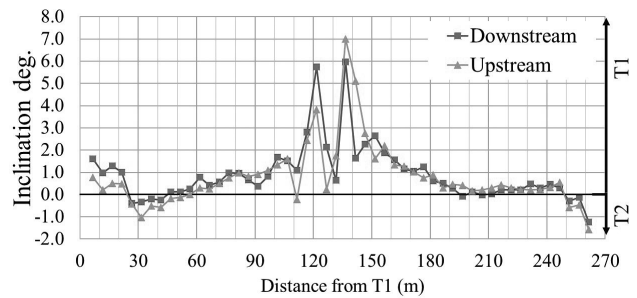


Fig. 10. Measurement of hanger inclination from TLS point cloud.

the three hangers closest to T2 were inclined toward T2. The rest of the hangers exhibited greater degree of inclination toward T1 tower as the location moved closer to the middle of the bridge deck. The inclination of the hanger ropes also indicated possible slippage of the clamp connecting each hanger to the main cables.

Step1 extracts the lower chord of the truss under each hanger. After visually inspecting the point cloud model, the deflection of the main deck cannot be measured from the road surface due to incomplete points. Hence, points from the lower chord were used. A reference point visible under T1 main tower was assumed to represent the normal elevation of the truss without sagging.

Step2 uses the lowest point from the extracted lower chord to represent the deflection of the truss.

Conventional measurement for truss deflection was carried out using automatic level on 16 October 2016 by MOC. The device provides accuracy of up to  $\pm 1.5$  mm

at 1 km double run leveling. The measurement was performed along the bridge deck at the expansion joint of T1 and T2 tower, as well as at each hanger rope. A total of 54 measuring points were obtained for each upstream and downstream.

### 3. Results and Discussions

#### 3.1. Point Cloud Registration

The final combined point cloud model for this study was completed with an average of 9.6 mm mean point co-registration error and average maximum point error of 15.37 mm. The final model was extracted into 3 sections, namely T1 tower, T2 tower, and hanger ropes. This reduced the number of points to be handled from 326 million points to approximately 20 million points for each extracted section. During the survey, it was observed that dust particles from sand surrounding the survey area sometimes blocked the rotating mirror of the scanner. Therefore, the rotating mirror was checked and cleaned if necessary. Without cleaning the mirror, these particles can produce noise in the final model. In addition, the object of interest is a suspension bridge, which was built to allow some structural movement. Consequently, the vibration of the bridge deck, especially toward the middle section, seems to affect the level of noise in the scan result and required manual cleaning. Data of the vibration behavior was not obtained, but it should be incorporated in future study.

#### 3.2. Tower Inclination Measurement

The inclination results of T1 and T2 are illustrated in Fig. 11. The deflection from both T1 and T2 indicated that the main towers on both sides are inclined toward the bridge axis direction. The displacements at the top were 21.4 cm and 30.7 cm at T1 and T2 respectively. The distribution of measured points along the height of both towers shows a higher degree curve shape as the height increases. Such behavior is expected when the condition at the bottom of the steel tower is fixed and the deformation is assumed to be a result of forces in the direction of the bridge deck acting at the top of the towers.

Inclination measurement using the conventional method was not available for either of the main towers at the Pathein Bridge. A simple method that can be employed are total station and inclinometer. The total station, while considered highly accurate, requires significant time and knowledge to collect large amount of data. On the other hand, the inclinometer suffers the limitation of discrete data collection. In this situation, TLS demonstrates clear advantages of providing data for the entire steel tower. This allows us to determine not only the level of inclination, but also its shape.

#### 3.3. Hanger Inclination Measurement

The shape of the inclined hanger ropes was expected to be curved similar to the deflection shape observed at

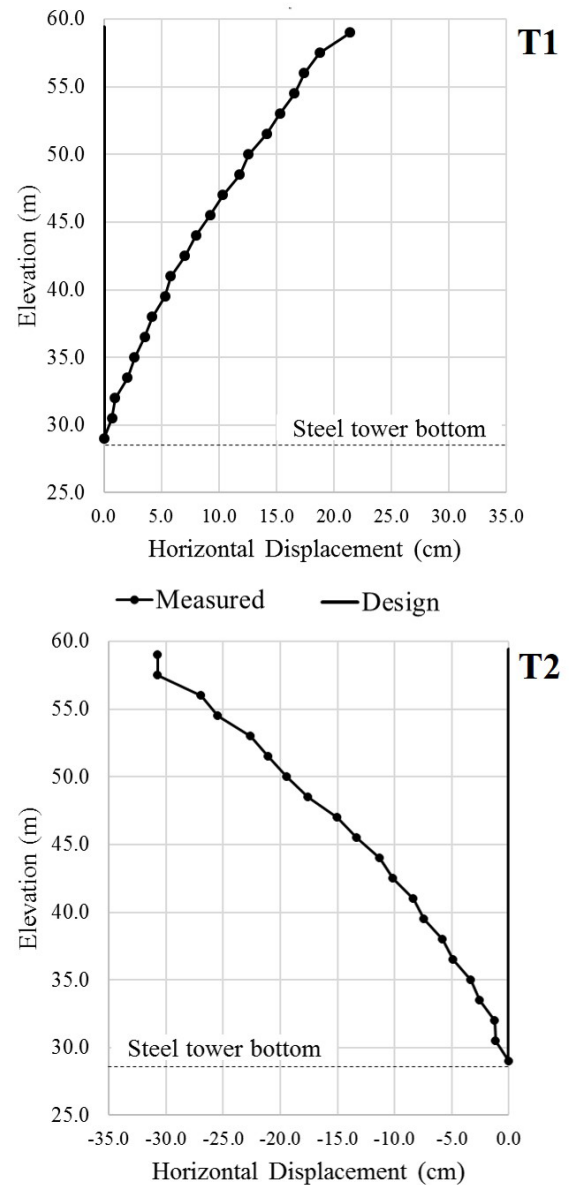
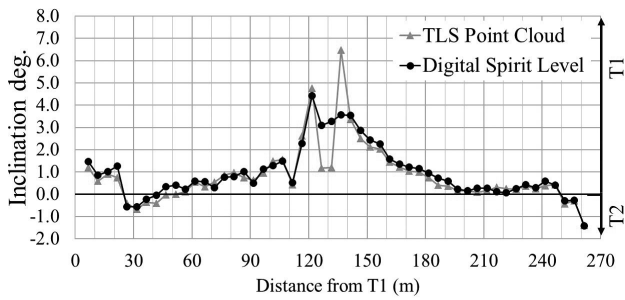


Fig. 11. Inclination of T1 and T2 tower measured from TLS point cloud.

tower T1 and T2. However, the missing points in some sections along the rope, especially the hangers located toward the middle section, prevented a clear shape to be extracted from the point cloud. Hence, the shape of the inclination was not presented in this study, but listed as observed limitation of TLS measurement.

The measured results were compared with conventional measurement from a hand-held digital spirit level. The measurements from the upstream and downstream sides were averaged and compared for both TLS data and digital spirit level. The comparison is presented in Fig. 12. Overall, the results showed good agreement. The average difference between the point cloud and data measured using the digital spirit indicated an underestimation of approximately 0.11 degree. A high discrepancy was observed in the middle of the main span. On closer inspection of the point cloud model, it was observed that



**Fig. 12.** Comparison of measurement from TLS and digital spirit level.

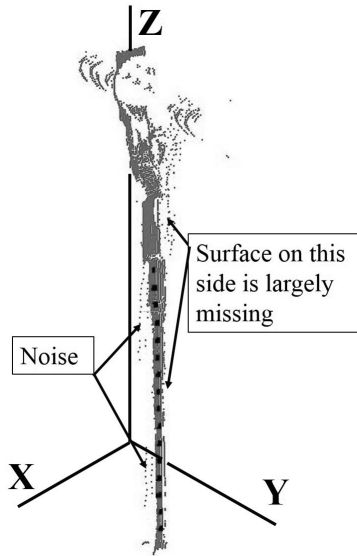


**Fig. 13.** Extracted sample of hanger rope with missing point and noises.

obstruction from the handrail resulted in some missing data at the bottom of the hanger ropes. In addition, increased vibration of the structure in the middle section likely caused higher uncertainty in the results. **Fig. 13** shows a segment of the hanger with missing surface point and noise. Hence, these errors were identified as limitations of the current point cloud model.

**3.4. Truss Deflection Measurement**

**Figure 14** presents the truss deflection of the main deck. Compared with the original design, the measurement identified significant differences, with the largest difference of 74.2 cm in the middle section of the deck. The deflection values closer to each tower showed greater sagging, with hangers nearer to T2 exhibiting the highest level of deflection. It is possible that the inclination of hangers presented in Section 3.3 can partially impact the deflection of the bridge deck. The slippage of clamps, though not measured in this study, was also observed by MOC during the field survey. Since the reasons for hanger inclination and slippage of clamps are not clear, neither can be excluded as a potential cause of deflection.

The elevation of road surface measurement using automatic level carried out in October 2016, 6 months prior

to TLS measurement, was compared with TLS measurement. The overall deflection between the two measurements showed a similar shape with less sagging effect measured from TLS point cloud. Similar to the hanger inclination results, measurements from the middle of the main span showed the highest difference. Two possible reasons for the differences between TLS and leveling measurements are recovery after concrete blocks removal and the difference in the measuring location. Since data collection by automatic level was performed right after the removal of the heavy concrete block on the main span [18], the recovery from additional load removal in 2016 was not as settled as during TLS survey. Another explanation is measurement location. Leveling measurement was carried out on top of the road surface. On the other hand, measurement from TLS point cloud used the bottom truss section to capture the deflection behavior. This section was scanned from the ground level at each side of the river bank. The distance from the scanner to the bottom truss, especially the middle section, resulted in the lowest part of the truss not being captured completely. We identified noise on some of the extracted lower chord, which can lead to differences in the result. Although errors from point cloud data itself cannot be clearly distinguished from the recovery effect, it can contribute to the difference and should be considered for future prevention of such effect.

**4. Conclusion**

This study aimed to examine the application of TLS technology for the measurement of suspension bridge deformation. Survey of the current geometric data from the bridge structure is important for structural analysis and maintenance decision. In this study, simple measurement techniques were used on direct output in point cloud format. Three deformation behaviors were selected including main tower inclination, hanger inclination, and deflection of truss. The findings of the study are summarized below.

- 1 Besides manufacturing errors, which varies depending on the device built and model, the uncertainty of TLS point cloud was also influenced by external factors during the field survey. These factors observed during this study include dust particles, the distance between object and scanner, vibration of structure, and occlusions. The average error from registering multiple scans to create a single point cloud was 9.6 mm. However, some locations can possess higher error up to 15.32 mm. An acceptable level of error depends on the objective. Higher accuracy can be achieved by minimizing the impact of aforementioned factors during field data collection. Hence, further research should be conducted in order to establish operational steps for TLS data collection.
- 2 The ability to provide non-discrete data, direct mea-

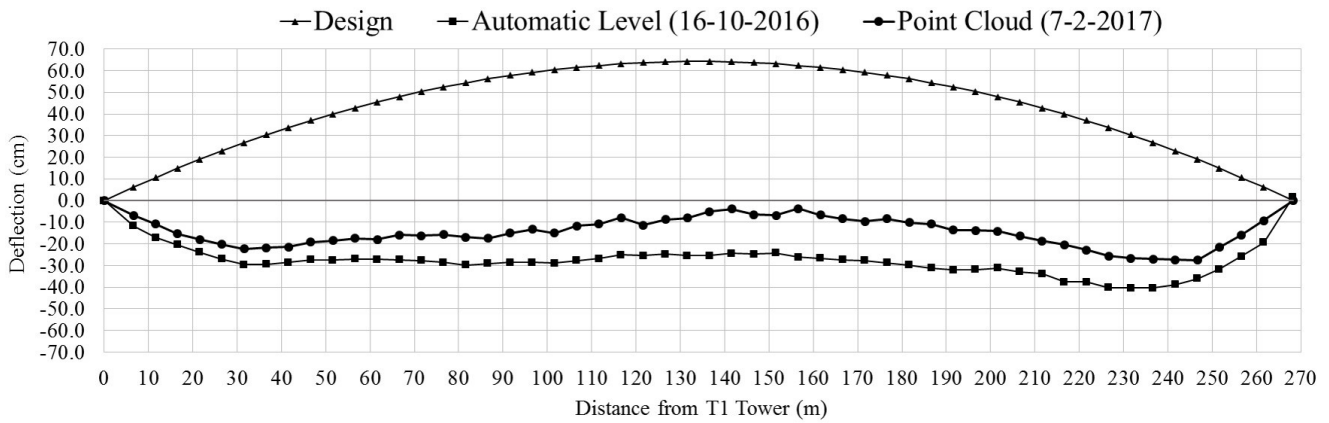


Fig. 14. Deflection of truss measured from TLS point cloud.

surement, and measurement of difficult-to-access areas were advantages of TLS technology observed in this study. Direct measurement can be carried out on TLS point cloud because it collects data in actual unit. The measurement of areas that are otherwise inaccessible or require extensive installation of other conventional devices, such as the entire main tower and main cable, can be done easily. These ability provide clear advantages over traditional visual inspection and recording using photographs. TLS utilizes a single device unlike the use of multiple measuring devices commonly required during inspection.

- 3 Limitations were also identified when measurement results from TLS were compared with available conventional measurement. High differences were observed at the middle section of the bridge deck. The observed errors were mostly due to the distance of objects from TLS, vibration of the structure, and occlusion. These factors should be considered during the planning stage, so that suitable scan locations can be selected to minimize errors.
- 4 This study utilized point cloud model, which considered the basic output from TLS survey. However, measurement results in some areas, such as the middle of the main span, showed high error due to noise and occlusion. An improved model can be generated by triangulating the point cloud into mesh or a CAD model. In such model, an interpolation algorithm can be applied to estimate missing data and exclude noise, in order to improve the final measurement.
- 5 Although structural analysis was not the focus of this study, we believe that the results can be used to further in order to identify possible causes of structural deformation and determine countermeasures to ensure structural safety.

#### Acknowledgements

This research was supported by the Japan Science and Technology Agency (JST)/ Japan International Cooperation Agency (JICA), Science and Technology Research Partnership for Sustainable Development Program (SATREPS). We would like to express our appreciation to Myanmar Ministry of Construction for their continuous support during field survey.

#### References:

- [1] Japan International Cooperation Agency, "Research Study on Review and Application of the Bridge Engineering Training Centre Project in Myanmar," Technical report, 2012.
- [2] Japan Infrastructure Partners, "Current Situation and Issues of Myanmar's Bridge Work," Technical report, Japan Infrastructure Partners, 2012, <http://www.infra-jip.or.jp/H23BridgeMaintenanceReportenglish.pdf> [accessed Sep. 17, 2016]
- [3] H. S. Park, H. M. Lee, H. Adeli, and I. Lee, "A New Approach for Health Monitoring of Structures: Terrestrial Laser Scanning," *Computer-Aided Civil and Infrastructure Engineering*, Vol.22, No.1, pp. 19–30, 2007, doi:10.1111/j.1467-8667.2006.00466.x.
- [4] W. Wang, W. Zhao, L. Huang, V. Vimarlund, and Z. Wang, "Applications of terrestrial laser scanning for tunnels: a review," *Journal of Traffic and Transportation Engineering (English Edition)*, Vol.1, No.5, pp. 325–337, 2014, doi:10.1016/S2095-7564(15)30279-8.
- [5] Y.-J. Cheng, W. Qiu, and J. Lei, "Automatic Extraction of Tunnel Lining Cross-Sections from Terrestrial Laser Scanning Point Clouds," *Sensors*, Vol.16, No.10, pp. 1648, 2016, <http://www.mdpi.com/1424-8220/16/10/1648>, doi:10.3390/s16101648.
- [6] T. Mill, A. Alt, and R. Liias, "Combined 3D building surveying techniques terrestrial laser scanning (TLS) and total station surveying for BIM data management purposes," *Journal of Civil Engineering and Management*, Vol.19, No.sup1, pp. S23–S32, 2013, <http://www.tandfonline.com/doi/abs/10.3846/13923730.2013.795187>, doi:10.3846/13923730.2013.795187.
- [7] V. Kankare, M. Holopainen, M. Vastaranta, E. Puttonen, X. Yu, J. Hyypä, M. Vaaja, H. Hyypä, and P. Alho, "Individual tree biomass estimation using terrestrial laser scanning," *ISPRS Journal of Photogrammetry and Remote Sensing*, Vol.75, pp. 64–75, 2013, <http://dx.doi.org/10.1016/j.isprsjprs.2012.10.003>, doi:10.1016/j.isprsjprs.2012.10.003.
- [8] S. Srinivasan, S. C. Popescu, M. Eriksson, R. D. Sheridan, and N. W. Ku, "Multi-temporal terrestrial laser scanning for modeling tree biomass change," *Forest Ecology and Management*, Vol.318, pp. 304–317, 2014, <http://dx.doi.org/10.1016/j.foreco.2014.01.038>, doi:10.1016/j.foreco.2014.01.038.
- [9] A. Pesci, G. Casula, and E. Boschi, "Laser scanning the Garisenda and Asinelli towers in Bologna (Italy): Detailed deformation patterns of two ancient leaning buildings," *Journal of Cultural Heritage*, Vol.12, No.2, pp. 117–127, 2011, <http://dx.doi.org/10.1016/j.culher.2011.01.002>, doi:10.1016/j.culher.2011.01.002.
- [10] M. J. Olsen, F. Kuester, B. J. Chang, and T. C. Hutchinson, "Terrestrial Laser Scanning-Based Structural Damage Assessment," *Journal of Computing in Civil Engineering*, Vol.24, No.3, pp. 264–272, 2010, doi:10.1061/(ASCE)CP.1943-5487.0000028.

- [11] G. Teza, A. Pesci, and A. Ninfo, "Morphological Analysis for Architectural Applications: Comparison between Laser Scanning and Structure-from-Motion Photogrammetry," *Journal of Surveying Engineering*, Vol.142, No.2014, pp. 1–10, 2016, doi:10.1061/(ASCE)SU.1943-5428.0000172.
- [12] W. Liu, S. Chen, and E. Hauser, "LiDAR-based Bridge Structure Defect Detection," pp. 27–34, 2011, doi:10.1111/j.1747-1567.2010.00644.x.
- [13] A. Pesci, G. Teza, E. Bonali, G. Casula, and E. Boschi, "A Laser Scanning-based Method for Fast Estimation of Seismic-induced Building Deformations," *ISPRS Journal of Photogrammetry and Remote Sensing*, Vol.79, pp. 185–198, 2013, doi:10.1016/j.isprsjprs.2013.02.021.
- [14] P. Oskouie, B. Becerik-Gerber, and L. Soibelman, "Automated Measurement of Highway Retaining Wall Displacements Using Terrestrial Laser Scanners," *Automation in Construction*, Vol.65, pp. 86–101, 2016, <http://dx.doi.org/10.1016/j.autcon.2015.12.023>, doi:10.1016/j.autcon.2015.12.023.
- [15] S. Sotoodeh, "Outlier Detection in Laser Scanner Point Clouds," *Iaprs*, Vol.XXX, No.Part 5, pp. 297–302, 2006.
- [16] R. Wahl and R. Klein, "Efficient RANSAC for Point-Cloud Shape Detection," *Computer Graphics Forum*, Vol.26, No.2, pp. 214–226, 2007.
- [17] T. Landes and P. Grussenmeyer, "Hough-Transform and Extended RANSAC Algorithms for Automatic Detection of 3D Building Roof from LiDAR Data," Vol.36, No.1, pp. 407–412, 2007.
- [18] Construction Myanmar Ministry of, "Pathein Report," Technical report, 2016.



**Name:**  
Nuntikorn Kitratporn

**Affiliation:**  
Master Course Student, The University of Tokyo

**Address:**

4-6-1 Komaba, Meguro-ku, Tokyo 153-8505, Japan

**Brief Career:**

2017 Graduated from Civil Engineering Department, University of Tokyo, Japan

2016-2017 President of International Student Association in Civil Engineering (ISACE), Civil Engineering Department, University of Tokyo

**Selected Publications:**

- N. Kitratporn, W. Takeuchi, K. Matsumoto, and K. Nagai, "Comparison of Close-range Structure-from-Motion Model from DSLR and Lightweight Wearable Camera for Bridge Inspection in Myanmar," In International Symposium on Remote Sensing, Nagoya, Japan, 2017.
- N. Kitratporn, W. Takeuchi, K. Matsumoto, and K. Nagai, "3D Structure-from-Motion Data Acquisition and processing for Twante Bridge Inclination Assessment," In 7<sup>th</sup> International Conference on Science and Engineering, Yangon, Myanmar, 2016.



**Name:**  
Wataru Takeuchi

**Affiliation:**  
Associate Professor, Institute of Industrial Science, The University of Tokyo

**Address:**

4-6-1 Komaba, Meguro-ku, Tokyo 153-8505, Japan

**Brief Career:**

2010-present Associate Professor, Institute of Industrial Science, The University of Tokyo 2010-2012 Director, Bangkok office, Japan Society for Promotion of Science (JSPS)

**Selected Publications:**

- P. Misra, A. Fujikawa, and W. Takeuchi, "Novel Decomposition Scheme for Characterizing Urban Aerosols Observed from MODIS," *Remote Sens.*, Vol.9, No.8, p. 812, 2017.
- T. Sritarapipat and W. Takeuchi, "Urban growth modeling based on the multi-centers of the Urban Areas and Land Cover Change in Yangon, Myanmar," *Journal of Remote Sensing Society of Japan*, Vol.37, No.3, pp. 248-260, 2017.
- M. Adachi, A. Ito, S. Yonemura and W. Takeuchi, "Estimation of Global Soil Respiration by Accounting for Land-use Changes Derived from Remote Sensing Data," *Journal of Environmental Management*, Vol.200, pp. 97-104, 2017.

**Academic Societies & Scientific Organizations:**

- American Society for Photogrammetry and Remote Sensing (ASPRS)
- Japan Society for Photogrammetry and Remote Sensing (JSPRS)



**Name:**  
Koji Matsumoto

**Affiliation:**  
Project Assistant Professor, Institute of Industrial Science, The University of Tokyo

**Address:**

4-6-1 Komaba, Meguro-ku, Tokyo 153-8505, Japan

**Brief Career:**

2010 Assistant Professor, Department of Civil Engineering, Tokyo Institute of Technology  
2015 Project Assistant Professor, International Center for Urban Safety Engineering, Institute of Industrial Science, the University of Tokyo

**Selected Publications:**

- H. Yokota, K. Nagai, K. Matsumoto and Y. Y. Mon, "Prospect for Implementation of Road Infrastructure Asset Management," *Advanced Engineering Forum*, Vol.21, pp. 366-371, 2017.
- P. Limpaninlachat, K. Matsumoto, T. Nakamura, K. Kono, and J. Niwa, "Flexural Strengthening Effect of Pre-tensioned UFC Panel on Reinforced Concrete Beams," *Journal of JSCE*, Vol.4, pp. 181-196, 2016.
- K. Matsumoto, T. Wang, D. Hayashi, and K. Nagai, "Investigation on the Pull-out Behavior of Deformed Bars in Cracked Concrete," *Journal of Advanced Concrete Technology*, Vol.14, pp. 573-589, 2016.
- L. Eddy, K. Matsumoto, and K. Nagai, "Effect of Perpendicular Beams on Failure of Beam-column Knee Joints with Mechanical Anchorages by 3D RBSM," *Journal of Asian Concrete Federation*, Vol.2, No.1, pp. 56-66, 2016.
- J. Niwa, Fakhruddin, K. Matsumoto, Y. Sato, M. Yamada, and T. Yamauchi, "Experimental Study on Shear Behavior of the Interface between Old and New Deck Slabs," *Engineering Structures*, ELSEVIER, Vol.126, pp. 278-291, 2016.

**Academic Societies & Scientific Organizations:**

- Japan Society of Civil Engineers (JSCE)
- Japan Concrete Institute (JCI)



**Name:**  
Kohei Nagai

**Affiliation:**  
Associate Professor, Institute of Industrial Science,  
The University of Tokyo

**Address:**  
4-6-1 Komaba, Meguro-ku, Tokyo 153-8505, Japan

**Brief Career:**  
2007 Assistant Professor, The University of Tokyo 2011 Associate  
Professor, The University of Tokyo

**Selected Publications:**

- L. Eddy and K. Nagai, "Numerical Simulation of Beam-column Knee Joints with Mechanical Anchorages by 3D Rigid Body Spring Model," Engineering Structures, Vol.126, pp. 547-558, 2016.

**Academic Societies & Scientific Organizations:**

- Japan Society of Civil Engineers (JSCE)

---